The Protein Journal (2020) 39:542–553
https://doi.org/10.1007/s10930-020-09910-3

Effects of Distal Mutations on Prolyl-Adenylate Formation of *Escherichia coli* Prolyl-tRNA Synthetase

Jonathan Zajac[1] · Heidi Anderson[1] · Lauren Adams[1] · Dechen Wangmo[1] · Shanzay Suhail[1] · Aimee Almen[1] · Lauren Berns[1] · Breanna Coerber[1] · Logan Dawson[1] · Andrea Hunger[1] · Julia Jehn[1] · Joseph Johnson[1] · Naomi Plack[1] · Steven Strasser[1] · Murphi Williams[1] · Sudeep Bhattacharyya[1] · Sanchita Hati[1]

Published online: 17 July 2020

Abstract

Enzymes play important roles in many biological processes. Amino acid residues in the active site pocket of an enzyme, which are in direct contact with the substrate(s), are generally believed to be critical for substrate recognition and catalysis. Identifying and understanding how these "catalytic" residues help enzymes achieve enormous rate enhancement has been the focus of many structural and biochemical studies over the past several decades. Recent studies have shown that enzymes are intrinsically dynamic and dynamic coupling between distant structural elements is essential for effective catalysis in modular enzymes. Therefore, distal residues are expected to have impact on enzyme function. However, few studies have investigated the role of distal residues on enzymatic catalysis. In the present study, the effects of distal residue mutations on the catalytic function of an aminoacyl-tRNA synthetase, namely, prolyl-tRNA synthase, were investigated. The present study demonstrates that distal residues significantly contribute to catalysis of the modular *Escherichia coli* prolyl-tRNA synthetase by maintaining intrinsic protein flexibility.

Keywords Aminoacyl-tRNA synthetase · Prolyl-tRNA synthetase · Non-catalytic residue · Dynamut · Protein flexibility

Abbreviations

ARS	Aminoacyl-tRNA synthetase
Ec	*Escherichia coli*
INS	Insertion domain
PBL	Proline-binding loop
Pro-AMP	Prolyl-adenylate
ProRS	Prolyl-tRNA synthetase
WT	Wild-type

1 Introduction

Aminoacyl-tRNA synthetases (ARSs) are essential enzymes that catalyze the covalent attachment of amino acids to their cognate transfer-RNA (tRNA). This reaction is known as the aminoacylation of tRNA and is a crucial step in protein synthesis in all living organisms. ARSs are large proteins, comprised of multiple domains [1]. Structural and biochemical characterization of the active sites of many enzymes, including ARSs, has revealed that only a small percentage (< 2%) of residues are directly involved in substrate binding and catalysis [2, 3]. It is not yet fully understood why ARSs are so large when only a small number of residues are directly involved in substrate recognition and catalysis. Earlier studies from our group revealed that various structural elements of ARSs are dynamically coupled [4–6], and coupled motions are correlated to the catalytic efficiency of ARSs. Recent studies on enzyme systems such as protein kinase A, nitrile hydratase, and alkaline phosphatase revealed that residues distal to the active site also participate in the biochemical function and assist enzymes to achieve their catalytic power [3, 7]. In the present study, we investigated the

Electronic supplementary material The online version of this article (https://doi.org/10.1007/s10930-020-09910-3) contains supplementary material, which is available to authorized users.

✉ Sanchita Hati
hatis@uwec.edu

[1] Department of Chemistry, University of Wisconsin-Eau Claire, Eau Claire, USA

role of distal residues on the catalytic function of the ARS, prolyl-tRNA synthetase.

Prolyl-tRNA synthetases (ProRSs) are class II synthetases that are responsible for ligating proline to $tRNA^{Pro}$ in a two-step reaction:

$$\text{Pro} + \text{ATP} + \text{ProRS} \rightleftharpoons \text{Pro-AMP} \cdot \text{ProRS} + \text{PP}_\text{i} \quad (1)$$

$$\text{Pro-AMP} \cdot \text{ProRS} + \text{tRNA}^{\text{Pro}} \rightarrow \text{Pro-tRNA}^{\text{Pro}} + \text{AMP} + \text{ProRS} \quad (2)$$

ProRSs from all three kingdoms of life are known to misactivate noncognate alanine and cysteine, which results in the formation of mischarged alanyl- and cysteinyl-$tRNA^{Pro}$ [8–10]. To maintain high fidelity in protein synthesis, some ProRSs have acquired pre- and/or post-transfer editing mechanisms to prevent misaminoacylation of $tRNA^{Pro}$ [9–11]. Based on sequence alignments, ProRSs are classified into two broad groups—"eukaryotic-like" and "prokaryotic-like" [12, 13]. *Escherichia coli* (Ec) ProRS, a representative member of the prokaryotic-like group, is a multi-domain protein like most ARSs (Fig. 1). The catalytic domain (motifs 1, 2 and 3; residues 64–81, 128–164, and 435–465) catalyzes the activation of proline and the aminoacylation of $tRNA^{Pro}$; the anticodon binding domain (residues 506–570) is critical for recognition of cognate tRNA; the insertion domain (also known as editing domain) (INS; residues 224–407, located between motifs 2 and 3 of the catalytic domain) is the post-transfer editing active site that hydrolyzes mischarged Ala-$tRNA^{Pro}$ [14, 15]. In contrast to the Ec ProRS INS domain, some species have a free-standing editing domain known as YbaK that hydrolyzes Cys-$tRNA^{Pro}$ [16, 17]. Furthermore, unlike prokaryotic-like ProRSs, eukaryotic-like ProRSs do not possess an INS domain, but in some cases, encode free-standing editing domain homologs [18].

In addition to post-transfer editing, the INS domain of Ec ProRS also assists in amino acid binding and activation [19]. Deletion of the editing domain (residues 232–394) of Ec ProRS resulted in a 200-fold increase in the K_M for proline and the overall efficiency of proline activation was reduced by ~ 1200-fold relative to the wild-type (WT) enzyme [19]. Previous studies have established that coupled domain dynamics play an important role in catalytic function of the multi-domain Ec ProRS [5]. More specifically, the anticorrelated motion between the INS domain and the catalytic domain is believed to assist in substrates binding and product release [20]. It has also been shown that the catalytically important proline-binding loop (PBL), which undergoes substantial conformational change upon substrate binding [21], is engaged in correlated motions with catalytic domain elements and anticorrelated motions with the INS domain [5]. Although dynamic coupling between these structural elements is crucial for Ec ProRS function, the role of many "non-catalytic" distal residues that are not directly involved in substrate recognition and binding has remained unexplored. In the present study, the effect of a select few "non-catalytic" distal amino acid residues on the catalytic activity of Ec ProRS was investigated. In particular, three sets of residues were investigated for their impact on enzymatic function: (i) the hinge residues (ALA238 and VAL391), (ii) residues in the vicinity of or within the PBL (THR199, SER201, and HIS208), and (iii) the non-catalytic residues that are proposed to be involved in maintaining coupled dynamics between INS and the catalytic domain (LEU281, LEU304, and VAL411) (Fig. 1) [6]. The two hinge residues between the INS domain and the catalytic domain of Ec ProRS, ALA238 and VAL391, were chosen to explore how the substitution of these two distant residues with a bulky or a small amino acid impacts the protein flexibility and catalysis. Similarly, it was unclear how much influence the polar residues that exist in the vicinity of the PBL, like THR199, SER201, and HIS208, have on catalysis. Also, the mutational effect of coevolved nonpolar residues like LEU281, LEU304, and VAL411 in bacterial ProRSs family [6], which are not directly involved in the two-step aminoacylation reaction but promote dynamic coupling between domains, remained unknown. Therefore, in the present study, site-directed mutagenesis and kinetic studies were performed to examine the impact of these distal residues on the prolyl-adenylate formation (Eq. 1) and aminoacylation of $tRNA^{Pro}$ (Eq. 2). Mostly alanine-scanning mutagenesis was carried out except for two cases; ALA238 and VAL391 (the two hinge residues) were substituted with a bulky proline and a small glycine, respectively. Changes in protein stability and flexibility were also analyzed using molecular simulations to examine if site-directed mutations of distal residues had any effect on dynamics, which is correlated to the catalytic rate. The results of the present study suggest that residues distal from the active site contribute significantly to the catalytic activity of Ec ProRS.

2 Methods

2.1 Materials

Proline, ATP, and other reagents including metal salts and buffers were from Sigma (> 99% pure). [γ-^{32}P]-ATP and [^{32}P]-PP_i were from Perkin Elmer. Primers for site-directed mutagenesis and PCR were from Integrated DNA Technologies. Inorganic pyrophosphatase (PP_iase) and reagents for in vitro transcription were from Fisher Scientific.

2.2 Enzyme Preparation

Overexpression and purification of histidine-tagged WT and mutant Ec ProRS were performed as described

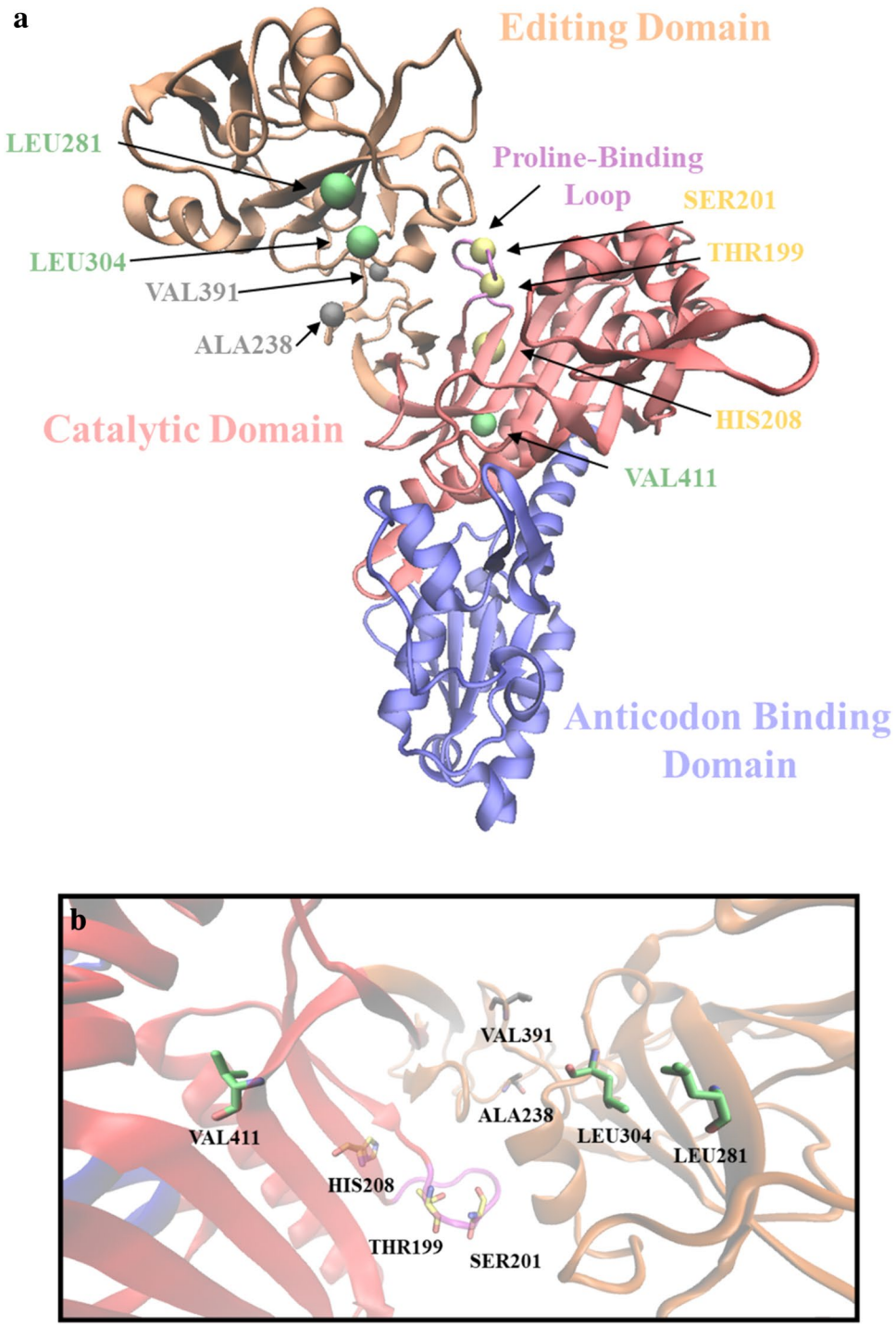

Fig. 1 Structural model of *E. coli* ProRS. Homology model was derived from *P. aeruginosa* ProRS. **a** The editing domain, proline-binding loop, catalytic domain, and anticodon binding domain are shown in orange, pink, red, and blue, respectively. **b** Distal residues that are probed for their role in catalysis. Hinge residues include ALA232 and VAL391 (shown in black spheres). Proline-binding loop residues include HIS208, SER201, and THR199 (shown in yellow spheres). Coevolving residues include LEU281, LEU304, and VAL411 (shown in green spheres) (Color figure online)

previously [22, 23]. Plasmids encoding T199A, S201A, H208A, A238P, L281A, V391G, L304A and V411A Ec ProRS were generated by site-directed mutagenesis of pCS-M1S [23] using primers listed in Table S1. Results of mutagenesis were confirmed by DNA sequencing (University of Wisconsin, Biotechnology Center-Madison). Protein expression was induced in Ec SG13009 (pREP4) competent cells with 0.1 mM isopropyl b-D-thiogalactoside for 4 h at 37 °C. Histidine-tagged proteins were purified using a Talon cobalt affinity resin and eluted with 100 mM imidazole. Protein concentrations were determined initially by the Bio-Rad assay (Bio-Rad Laboratories) followed by active-site titration [24].

2.3 RNA Preparation

Ec $tRNA^{Pro}$ was transcribed using T7 RNA polymerase from BstN1-linearized plasmid as described [25] and purified by denaturing 12% polyacrylamide gel electrophoresis.

2.4 Enzyme Assays

The ATP-PP_i exchange assay was performed at 37 °C according to the published method [26]. The concentrations of proline ranged from 0.05 to 2 mM. The enzyme concentrations used were 10–40 nM for proline activation. Kinetic parameters were determined from Lineweaver–Burk plots and represent the average of at least three determinations.

Aminoacylation assays were performed following the procedure described by Cestari and Stuart [27] at 37 °C in a reaction mixture containing 30 mM HEPES (pH 7.5), 140 mM NaCl, 30 mM KCl, 40 mM $MgCl_2$, 1 mM DTT, 0.2 mM ATP, 2 mM proline, 2 µ/ml inorganic pyrophosphatase (PP_iase), 8 mM $tRNA^{Pro}$, and 4 mM WT and mutant variants of Ec ProRS. Briefly, the two-step aminoacylation reactions (50 ml) were conducted in 96-well plates and measured the amount of inorganic phosphate that was formed due to the cleavage of pyrophosphate in the presence of inorganic phosphatase. Aminoacylation reactions were incubated for 30 min at 37 °C and then quenched by the addition of malachite green solution (100 ml), which reacts with the inorganic phosphate to give a shade of green. The absorbances of the solutions were measured at 620 nm to determine the amount of inorganic phosphate formed, which correlates with the amount of prolyl-$tRNA^{Pro}$ formed.

2.5 Homology Modeling

PSI-BLAST [28] was used to identify a reliable template to build a three-dimensional model structure of Ec ProRS. Homology modeling was carried out using Swiss Model and *Pseudomonas aeruginosa* ProRS (PDB code: 5UCM) as a template [29, 30].

2.6 Flexibility Analysis

The impact of point mutations on Ec ProRS stability and flexibility was analyzed using the web server—DynaMut [31]. DynaMut employs normal mode analysis and provides an assessment of the effect of a point mutation on a protein's stability and flexibility. DynaMut utilizes two approaches, Bio3D and a coarse-grained elastic network contact model (ENCoM) and enables rapid analysis of the effect of point mutations on protein flexibility ($\Delta\Delta S$) and stability ($\Delta\Delta G$) resulting from vibrational entropy changes [31]. For assessing the effects of mutations on protein flexibility and stability, the server requires the PDB file or PDB accession code of the protein and the point mutation is specified as a string containing the WT residue one-letter code, its corresponding residue number, and the mutant residue one-letter code.

2.7 Protein Visualization

The 3D model generated from Swiss Model was visualized through Visual Molecular Dynamics (VMD) software [32]. The WT protein and locations of the mutations were analyzed to examine possible interactions between the targeted residues with their neighboring residues and the effect of mutations on those noncovalent interactions.

3 Results

3.1 Homology Modeling

PSI-BLAST [28] search resulted in a pairwise alignment of the Ec ProRS (target protein) with the prolyl-tRNA synthetase from *Pseudomonas aeruginosa* (PDB ID: 5UCM), which served as the template protein for the homology modeling. Pairwise sequence alignment showed 71% identities and 83% similarities. Using the template protein and Swiss-Model [29], the three-dimensional model structure of 577-residue Ec ProRS was developed (Fig. 1). The structural assessment of the model yielded a global model quality estimation (GMQE) value of 0.86 (Table 1); GMQE score is expressed as a number between 0 and 1, higher numbers indicate higher reliability [30]. Also, QMEAN, which measures the "degree of nativeness," i.e. how comparable the model structure is to the experimental structure, was − 0.56 for the model structure [30]. A QMEAN Z-score close to zero indicates good agreement between the model structure and experimental structures of similar size [30]. Pairwise structural alignment using DALI [33] resulted in an RMSD of 0.2 Å and a Z-score of 57.3; a higher value of DALI Z-score indicates greater similarity between two protein structures (Table 1). Stereochemical parameters analyzed for the target protein showed 95.51% residues with favorable dihedral angles (Ramachandran favored), 0.88% residues with non-favorable dihedral angles (Ramachandran outliers), 1/9098 unfavorable bonds, and 25/12328 unfavorable angles. Stereochemical analysis of the template protein resulted in 97.15% residues with favorable dihedral angles, 0.0% residues with non-favorable dihedral angles, 1/8814 unfavorable bonds, and 3/11970 unfavorable angles (Table 1, Fig. S1). Taken together, the structure assessment results suggested that the model structure of Ec ProRS is reliable.

Table 1 Homology and stereochemical parameters of the homology model structure of Ec ProRS and template protein structure [ProRS of *Pseudomonas aeruginosa* (PDB ID: 5UCM)]

Homology parameter		Value
SWISS Model QMEAN		−0.56
SWISS Model GMQE		0.86
DALI RMSD		0.20
DALI Z-Score		57.3
Stereochemical parameter	Homology model	Template (5UCM)
Ramachandran favored	95.51%	97.15%
Ramachandran outliers	0.88%	0.00%
Bad bonds	1/9098	1/8814
Bad angles	25/12328	3/11970

Table 2 Steady state kinetic parameters for proline activation by wild-type and mutant variants of Ec ProRS

ProRS	K_M (mM)	k_{cat} (s^{-1})	k_{cat}/K_M (s^{-1} mM^{-1})	Fold-decrease
WT	0.392 ± 0.001	9.1 ± 0.9	23. ± 2	1.0
A238P	1.6 ± 0.2	5.6 ± 0.4	3.5 ± 0.5	6.6
V391G	1.9 ± 0.1	4.5 ± 0.6	2.4 ± 0.3	9.6
T199A	3.1 ± 0.8	2.4 ± 0.5	0.77 ± 0.3	29.9
S201A	0.703 ± 0.008	5.4 ± 0.4	7.7 ± 0.6	3.0
H208A	4.9 ± 0.4	1.8 ± 0.1	0.37 ± 0.03	62.2
L281A	2 ± 0.5	5.5 ± 0.8	3 ± 1	7.7
L304A	0.17 ± 0.01	1.9 ± 0.2	11. ± 1.3	2.1
V411A	2.0 ± 0.2	4.5 ± 0.4	2.2 ± 0.3	10.5

3.2 Proline Activation

To explore the role of the distal residues on ProRS functions, site-directed mutagenesis of a few selected distal residues was conducted. Steady-state kinetics were performed to examine the impact of mutations on proline activation. The impact of single-point mutations on protein flexibility was analyzed using Dynamut [31].

3.2.1 Hinge Residues (ALA238 and VAL391)

Two hinge residues of Ec ProRS were subjected to mutagenesis. Proline activation efficiency (k_{cat}/K_M) was reduced by 6.6- and 9.6-fold for A238P and V391G,

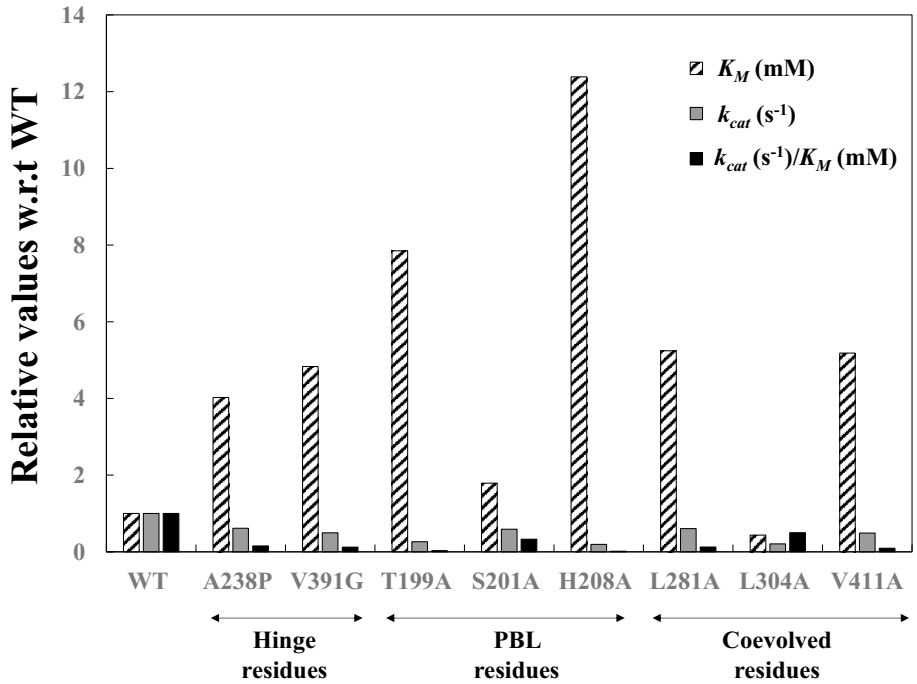

Fig. 2 Comparison of kinetic parameters. K_M, k_{cat}, and k_{cat}/K_M for Pro-AMP formation by WT and mutant variants of Ec ProRS. Relative K_M, k_{cat} and k_{cat}/K_M displayed on the y-axis were normalized to the K_M, k_{cat} and k_{cat}/K_M values of WT enzyme. The average values and standard deviations are reported in Table 2

Table 3 Impact of mutation of distant residues on protein stability ($\Delta\Delta G$) and flexibility ($\Delta\Delta S$)

ProRS	$\Delta\Delta G$ (kcal mol^{-1})	$\Delta\Delta S$ (kcal mol^{-1} K^{-1})
WT	–	–
A238P	0.521	−0.514
V391G	−0.760	0.381
T199A	−0.796	0.498
S201A	0.447	−0.126
H208A	−1.125	0.501
L281A	−0.458	0.446
L304A	−2.447	0.532
V411A	−2.867	0.544

respectively (Table 2 and Fig. 2). The K_M for proline was increased by ~ four–fivefold for these two mutant variants. There was a significantly less impact on k_{cat}, which was decreased only by ~ 0.5-fold for A238P and V391G compared to WT enzymes (Table 2). The substitution of alanine with a bulky proline (A238P) caused a decrease in flexibility ($\Delta\Delta S = -0.514$ kcal mol^{-1} K^{-1}), whereas substitution of valine with glycine (V391G) resulted in an increase in protein flexibility ($\Delta\Delta S = 0.381$ kcal mol^{-1} K^{-1}) (Table 3). A238P was found to be a stabilizing mutation ($\Delta\Delta G = 0.521$ kcal mol^{-1}), while V391G was destabilizing ($\Delta\Delta G = -0.760$ kcal mol^{-1}) (Table 3).

3.2.2 PBL Residues (THR199, SER201, and HIS208)

Three residues within the PBL region of Ec ProRS—THR199, SER201, and HIS208—were mutated to alanine. Reduced catalytic efficiency of proline activation was observed for all three mutants, but to a lesser degree for S201A (Table 2). The K_M for T199A was increased by eightfold, k_{cat} was decreased by fourfold, and the k_{cat}/K_M was decreased by 30-fold with respect to WT enzyme (Table 2 and Fig. 2). In the S201A mutant, the K_M was increased by twofold, k_{cat} was decreased by ~ twofold, and the k_{cat}/K_M was reduced only by threefold relative to the WT enzyme (Table 2, Fig. 2). In the H208A mutant, the $K_M$was increased 12-fold, k_{cat} was decreased fivefold, and the k_{cat}/K_M was drastically decreased by 62-fold (Table 2 and Fig. 2). The alteration in protein flexibility was less for S201A ($\Delta\Delta S = -0.126$ kcal mol^{-1} K^{-1}) compared to T199A ($\Delta\Delta S = 0.498$ kcal mol^{-1} K^{-1}). S201A resulted in an overall stabilizing effect ($\Delta\Delta G = 0.447$ kcal mol^{-1}), while T199A resulted in an overall destabilizing effect ($\Delta\Delta G = -0.796$ kcal mol^{-1}). H208A caused overall destabilization ($\Delta\Delta G = -1.125$ kcal mol^{-1}) in the system as well as increased protein flexibility ($\Delta\Delta S = 0.501$ kcal mol^{-1} K^{-1}) (Table 3).

3.2.3 Coevolving Residues (LEU281, LEU304, and VAL411)

Substitution of alanine for leucine at positions 281 and 304 resulted in decreased catalytic efficiency (7.7- and 2.0-fold decrease, respectively) (Table 2 and Fig. 2). L304A was shown to cause destabilizing effects to a much greater degree than L281A ($\Delta\Delta G = -2.447$ kcal mol^{-1} vs. $\Delta\Delta G = -0.458$ kcal mol^{-1}). However, increase in protein flexibility ($\Delta\Delta S$) was comparable for both mutants (Table 3). V411A results in destabilization and an increase in protein flexibility ($\Delta\Delta G = -2.867$ kcal mol^{-1} and $\Delta\Delta S = 0.544$ kcal mol^{-1} K^{-1}), coinciding with a 10.5-fold decrease in catalytic efficiency (Table 2 and Fig. 2).

3.3 Aminoacylation of tRNA^{Pro}

The hinge mutants, A238P and V391G, had a 20% and 40% reduction in product (Pro-tRNA^{Pro}) formation, respectively, compared to WT enzyme (Fig. 3). Aminoacylation of tRNA^{Pro} was reduced by ~ 60% in the case of T199A, S201A, and H208A. A more drastic impact on product formation was observed for L281A and L304A with 70% and 80% reductions, respectively. V411A resulted in a 40% reduction in product formation. Taken together, the decreases in aminoacylation efficiency in mutant variants were 1.5- to fivefold due to single point mutation. In particular, there was a significant decrease in aminoacylation activity due to the mutation of residues in the PBL region and in the editing domain.

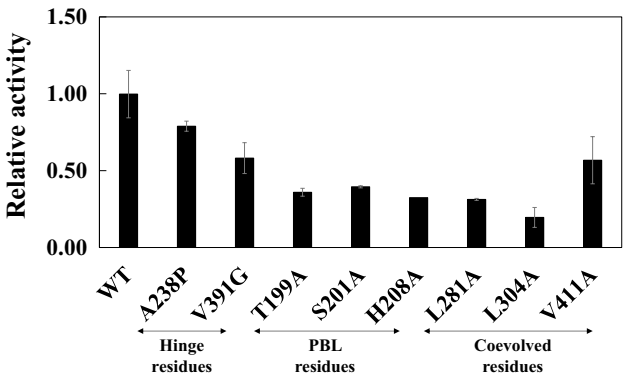

Fig. 3 Aminoacylation of tRNA^{Pro} with proline by WT and mutant variants of Ec ProRS. The assay was performed at 37 °C with 8 μM tRNA^{Pro} and 4 μM enzymes. These results are the average of three determinations for all but H208A; the percent error is 0.5 for H208A. Relative catalytic activities displayed on the y-axis were normalized to the activity of WT enzyme

4 Discussion

Proteins are intrinsically dynamic, and their conformational dynamics are intricately linked to their functions [34]. Earlier studies revealed that the editing domain of Ec ProRS is involved in anticorrelated motion with respect to the catalytic and anticodon binding domains, while intradomain motifs are mainly engaged in correlated motions [5, 20, 35]. Furthermore, coupled domain dynamics and domain-domain cross-talks are mediated by networks of interacting residues engaged in correlated motions [6]. Since these dynamics and cross-talks are essential for the function of Ec ProRS, it was hypothesized that distal residues would also contribute to enzyme catalysis. To test this hypothesis, several single-point mutant variants of Ec ProRS were constructed and their catalytic efficiencies in proline activation (Eq. 1) and aminoacylation (Eq. 2) were investigated.

4.1 Proline Activation

The impact of mutation of distal residues on proline activation efficiency was investigated. All mutants investigated had decreased proline activation efficiency, but several mutants showed significantly lower activation efficiencies compared to WT ProRS (Table 2). The impact of mutation of each of these distal residues are elaborated below.

4.1.1 Hinge Residues (ALA238 and VAL391)

The two hinge residues, ALA238 and VAL391, of Ec ProRS (Figs. 1 and 4) were identified using the web server HINGEprot for protein hinge prediction [36]. These residues were either made more rigid (A238P) or flexible (V391G) and their impact on prolyl-adenylate formation was assessed. Using the ATP-PP_i exchange reaction, we found that the alteration of the flexibility of these two hinge sites had significant impact on the catalytic efficiency of Ec ProRS. Earlier studies have shown that the INS domain and PBL loop is engaged in anticorrelated motions [5]. Any disruption in

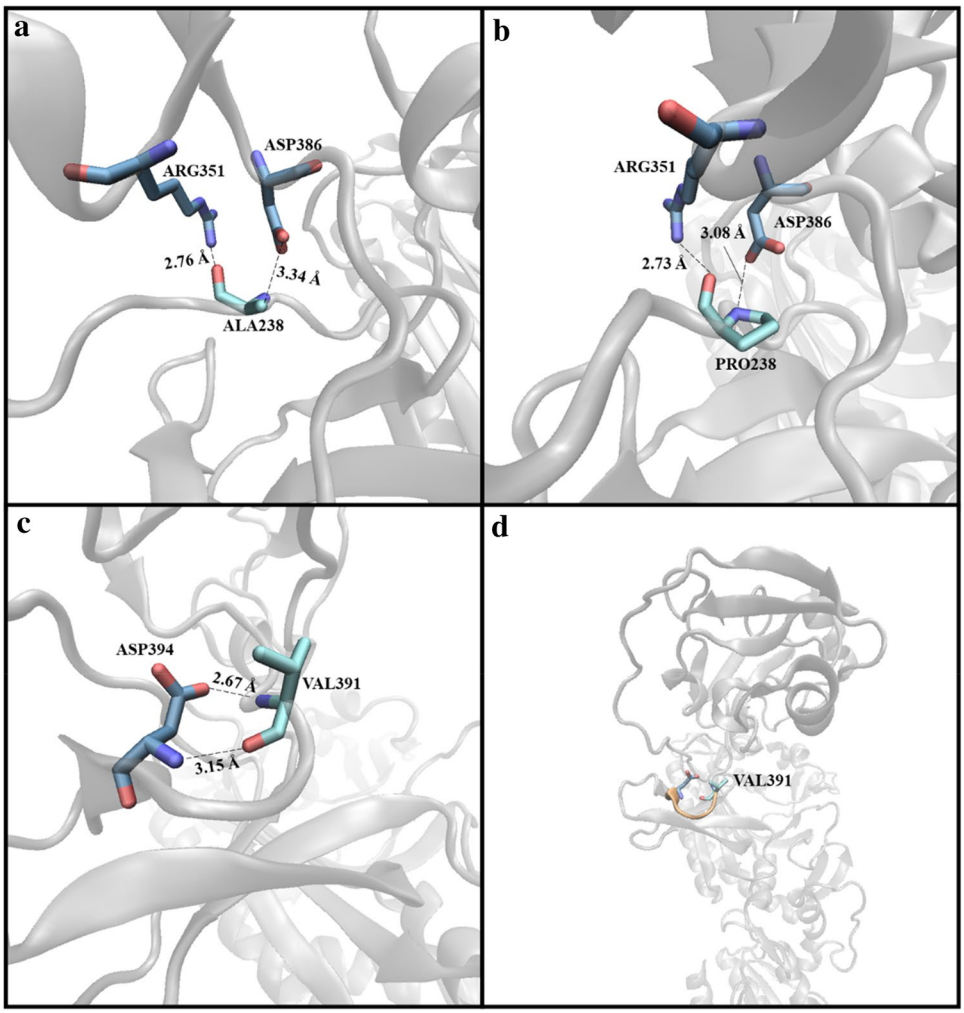

Fig. 4 A238P and V391G mutations. Key residues involved in noncovalent interactions with the hinge residues ALA238 and VAL391 are shown. **a** ALA238 is shown to interact with ARG351 and ASP386. **b** A proline substitution is shown to not significantly alter the interactions with residue 238. **c** VAL391 is shown to interact with ASP394. **d** Regions proposed to be impacted by a mutation of residue 391 are highlighted in orange. Residue 391 may play a key role in the stability of the loop from residues 391 to 394 (Color figure online)

the coupled motion between these two structural elements had impact on substrate binding. Introducing a bulky or a small amino acid at the hinges between the INS and catalytic domain (Fig. 1) results in alteration of the protein flexibility, as revealed from Dynamut analysis [31]. Stabilization due to the A238P mutation appears to reduce flexibility by substituting alanine with proline. Structural assessment suggests that ALA238 interacts with surrounding residues ARG351 and ASP386 via hydrogen bonding (Fig. 4a), and neither interaction appears to be compromised following a mutation to proline at residue 238 (Fig. 4b). The VAL391 residue involves in hydrogen bonding interactions with ASP394 (Fig. 4c). Substitution of glycine at position 391 did not alter these interactions. However, the substitution of the larger valine with the smaller glycine has increased the flexibility of the loop consisting of residues 391–394 (Fig. 4d). Despite the opposing nature of these mutations (reduced flexibility at position 238 and increased flexibility at position 391), catalytic efficiency was decreased in both cases. These results suggest that mutations of the hinge residues of Ec ProRS perturb the intrinsic flexibility of distal sites. More specifically, these mutations disrupt the mobility present in the WT enzyme that is conducive for substrate binding and catalysis is disrupted due to such mutations.

4.1.2 PBL Residues (THR199, SER201, and HIS208)

The proline-binding loop (residues 199–206) undergoes substantial conformational change upon substrate binding. In the absence of bound ligand, the PBL is in a disordered "open" conformation. In the presence of prolyl-adenylate, the loop undergoes a transition of 8 Å and attains a well-ordered "closed" conformation [21]. Structural analysis of prokaryote-like ProRSs has shown that two highly conserved flanking motifs, 174-YxxxxxAYxxxFxR-187 and 208-H/KEF-210, firmly anchor the PBL in the catalytic domain, which allows substantial movement upon substrate binding [21]. To investigate the role of residues in and around the PBL, which are not directly involved in substrate binding and catalysis, alanine-scanning mutation of three residues—THR199, SER201, and HIS208 was performed and the effect of mutations on catalytic activity was examined. The kinetic parameters for proline activation were determined for these mutants and compared with WT Ec ProRS. Analysis of protein flexibility and stability using DynaMut revealed that the mutation of PBL residues have more impact on catalysis if there is an increase in overall flexibility. Substitution of SER201 with alanine resulted in an increase in protein stability, likely due to the release of strain present in the WT enzyme. This decreased impact on the catalytic efficiency of S201A is believed to be due to less alteration in protein flexibility compared to T199A (Table 3). THR199 and SER201 are both implicated in the stability of the PBL, contributing to a network of interactions also including ASP198, GLY203, and LYS311 (Fig. 5). An alanine mutation of SER201 does not seem to significantly compromise these interactions (Fig. 5a, b), explaining the small change in flexibility and overall stabilizing effect. Substitution of THR199 with alanine, however, appears to eliminate the hydrogen bonding present in the WT (Fig. 5c, d). Decreased catalytic efficiency is likely due to destabilization and increased protein flexibility. HIS208 appears to be a crucial residue in the stability of a helix from residues 166–189 and interacts with two tyrosine residues (174 and 178) located on a prominent helix found within the catalytic domain (Fig. 6). These interactions are shown to be compromised following an alanine mutation at residue 208 (Fig. 6a, b). Thus, these PBL residues, even though not directly involved in any interactions with proline, favor substrate binding and prolyl-adenylate formation. Distal mutations have been shown to elicit similar effects on the activity of *E. coli* DinB (DNA polymerase IV) [37].

4.1.3 Coevolving Residues (LEU281, LEU304, and VAL411)

An earlier computational study demonstrated that the INS domain of prokaryotic-like ProRSs is engaged in coupled motion with various structural elements of the catalytic domain including the PBL [5]. The collective dynamics of the PBL were altered by the deletion of the INS or point mutation at the INS-aminoacylation domain junction [5]. Using statistical thermal coupling analysis, the pre-existing residue-residue interactions between the INS and aminoacylation domains of Ec ProRS that modulate PBL dynamics were identified [6]. Residues 281 and 304 appear to be implicated in a similar network of interactions, involving VAL298, PHE321, and ILE387 (Fig. 7a–e). Structural analysis reveals that LEU281 may favorably interact with ALA304 (Fig. 7c, d), limiting the decrease in catalytic efficiency following mutation. While both mutations resulted in increased flexibility, L304A caused destabilizing effects to a much greater degree than L281A (Table 3). LEU304 appears to be involved in interactions between two unique loops via PHE321 and ILE387 (Fig. 7c). Loss of contact with residues 321 and 387 may result in the observed increased flexibility and decreased stability. This suggests that the interactions between these distal LEU281 and LEU304 residues are crucial to proline activation, and concurrent mutations of both residues may result in an even more pronounced decrease in catalytic efficiency. V411A results in the most destabilizing effect and greatest change in flexibility of the tested mutations (Table 3). Residue 411 appears to be involved in the stabilization of helices from residues 166–189, similar to HIS208, as well as a smaller helix from residues 448–459 (Fig. 8). The combined results from H208A and V411A suggests that the catalytic domain helix from residues

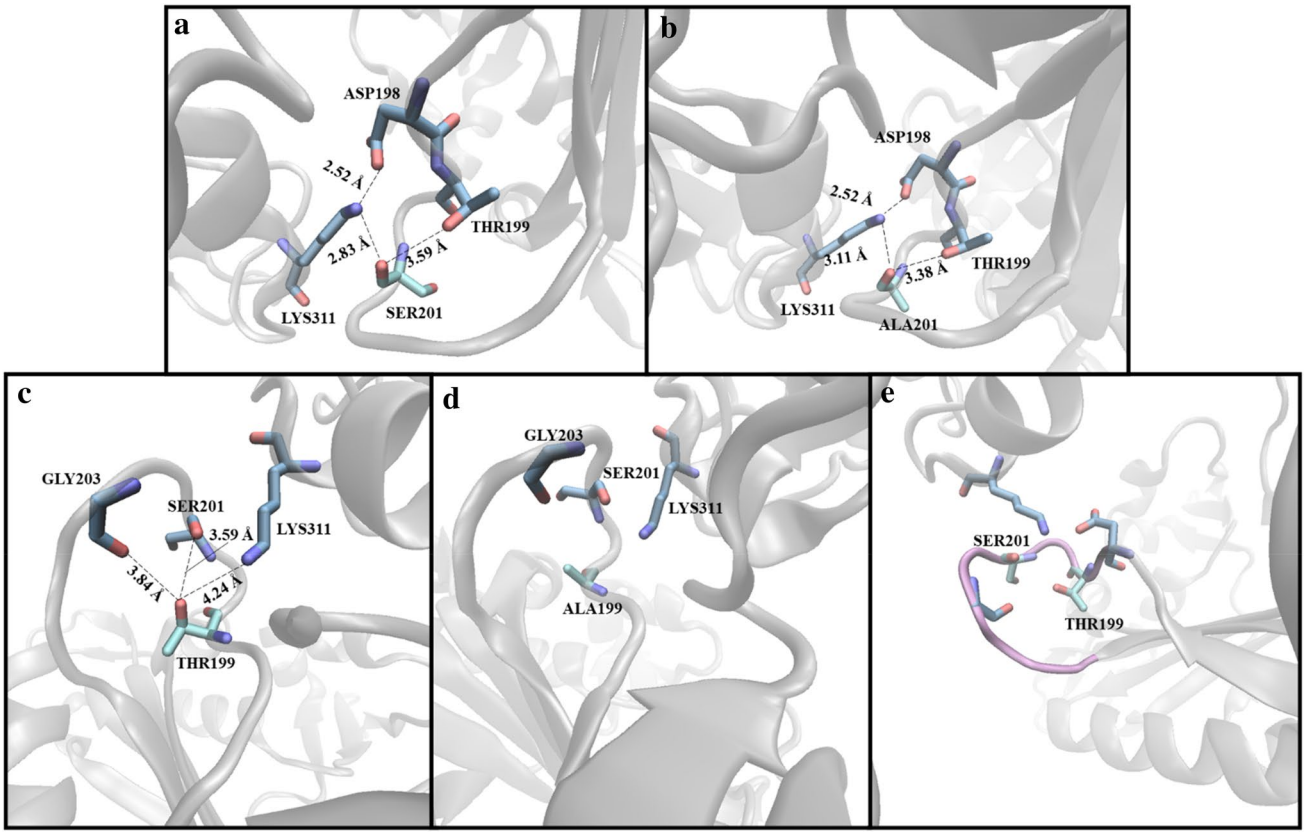

Fig. 5 S201A and T199A mutations. Key residues involved in the stabilization of the proline-binding loop are shown. **a** SER201 is shown to interact with LYS311, THR199, and ASP198. **b** An alanine substitution does not significantly alter the interactions present with residue 201. **c** THR199 is shown to interact with SER201, GLY203, and LYS311. **d** An alanine substitution at residue 199 results in complete loss of hydrogen bonding interactions at this site. Residue 199 may play a crucial role in the stabilization of the proline-binding loop. **e** The proline-binding loop, initially proposed to be impacted by mutations at residues 201 and 199, is shown in pink (Color figure online)

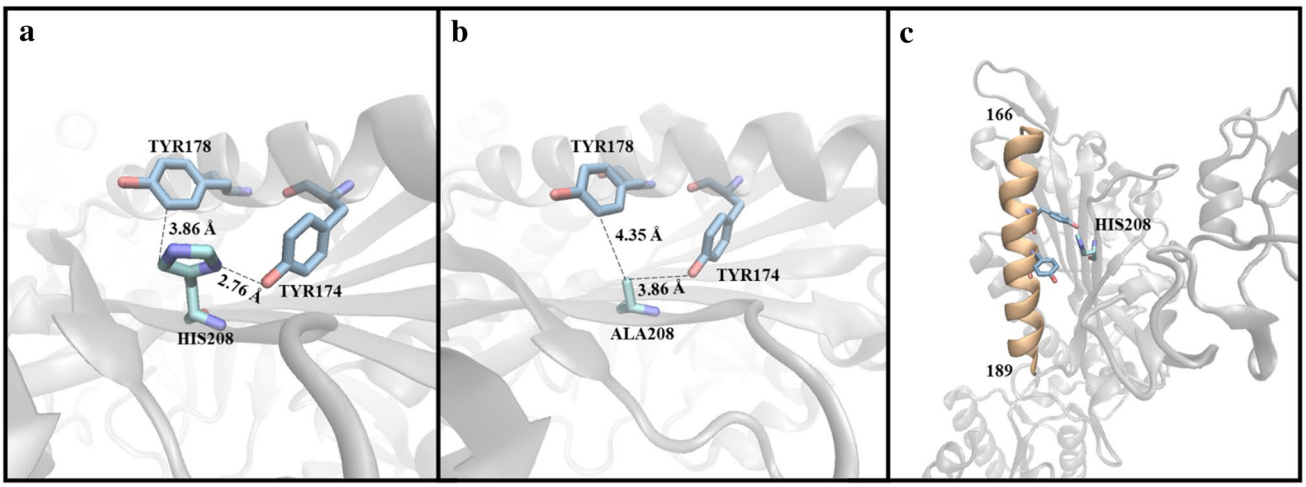

Fig. 6 H208A mutation. Key residues involved in noncovalent interactions with the PBL residue HIS208 are shown. **a** HIS208 is shown to interact with TYR178 and TYR174. **b** The mutation of residue 208 to alanine results in disruption in pi–pi interactions between HIS208, TYR178, and TYR174. **c** Regions proposed to be impacted by a mutation of HIS208 are highlighted in orange. Residue 208 may play a key role in bringing stability to the helix formed of residues 166–189 (Color figure online)

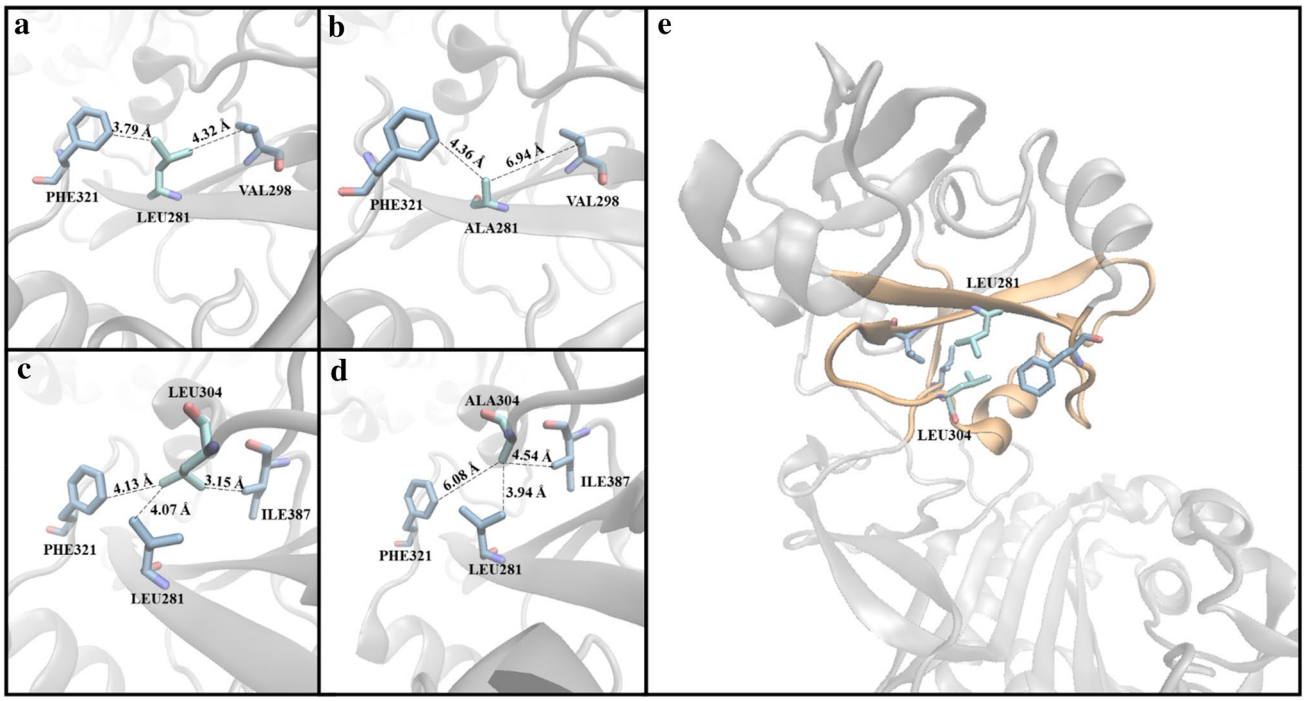

Fig. 7 L281A and L304A mutations. Key residues involved in the stabilization of the editing domain are shown. **a** LEU281 is shown to interact with PHE321 and VAL298. **b** An alanine substitution at residue 281 results in loss of contact with VAL298 and an increased distance from PHE321. **c** LEU304 is shown to interact with PHE321 and ILE387. **d** An alanine substitution at residue 304 results in loss of contact with PHE321 and an increased distance from ILE387. LEU281 may provide a compensatory effect, limiting the destabilizing effect of this mutation. **e** Regions proposed to be impacted by mutations at residues 281 and 304 are shown in orange (Color figure online)

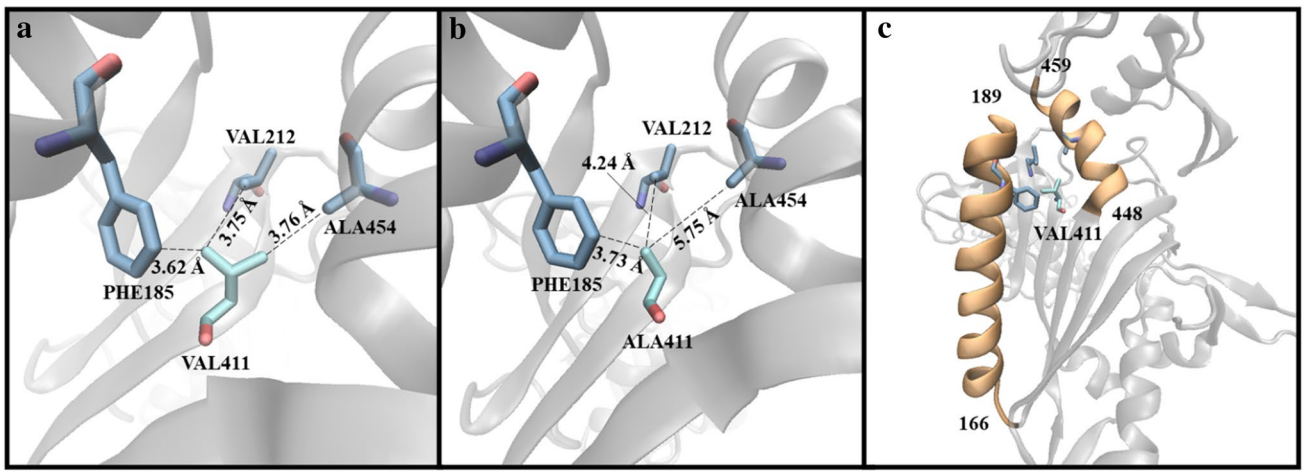

Fig. 8 V411A mutation. Key residues involved in noncovalent interactions with the coevolving residue VAL411 are shown. **a** VAL411 is shown to interact with PHE185, VAL212, and ALA454. **b** An alanine substitution at residue 411 results in an increased distance from PHE185, VAL212, and ALA454. **c** Regions proposed to be impacted by a mutation at residue 411 are highlighted in orange. Residue 411 may play a key role in the stability of helices from residues 166–189 and 448–459 (Color figure online)

166–189 plays a critical role in proline activation. Analyses of LEU281, LEU304, and VAL411 suggest that distal coevolving residues are involved in maintaining the overall stability and catalytic efficiency of Ec ProRS.

4.2 Aminoacylation of tRNA^{Pro}

As discussed earlier, the mutation of distal residues can impact protein flexibility and stability, thereby impacting

enzyme activity. This observation is reflected in the aminoacylation reaction results of the mutants studied here. A decrease in aminoacylation activity was observed for each of the eight mutants (Fig. 3). Alterations in the flexibility of the hinge residues, ALA238 and VAL391 had relatively less impact on Pro-tRNA^{Pro} formation. Mutations of residues in and around the PBL had significant impact on overall enzymatic function. A greater impact was observed for the mutation of two residues in the INS domain, which are believed to be important for domain-domain communication. These decreases in aminoacylation efficiency in the mutant variants strongly suggest that the distant residues are important for catalysis. Taken together, the present study suggests that perturbations at distant sites impact both prolyl-adenylation and aminoacylation reactions that take place at the catalytic domain. In particular, alteration in the protein flexibility due to a mutation resulted in decreased catalytic efficiency. In most cases, the catalytic efficiency decreased with the increase in flexibility in the mutant variants. The interplay between protein flexibility and catalytic efficiency is reported elsewhere [38].

5 Conclusions

By employing site-directed mutagenesis and steady-state enzyme kinetics, we found that mutations of distal residues have significant impact on the catalytic activity of Ec ProRS. Earlier studies have shown that the efficient aminoacylation of tRNA for most synthetases require communication between domains [39]. A previous study described how point mutations in the anticodon-binding domain of synthetases often lead to severely reduced catalytic efficiency [39]. In the present study, it was observed that the mutation of the two residues (LEU281 and LEU304) within the INS domain, which are known to be involved in maintaining coupled dynamics between domains, resulted in decreased proline activation and tRNA aminoacylation efficiencies. This observation highlighted the importance of distal residues in catalysis. Distal residues have been shown to affect the catalytic efficiency of other enzymes, in addition to ARSs. For example, single mutations outside the active site affect the substrate specificity of β-glycosidase [40]. Distal residues play an essential role in regulating human monoacylglycerol lipase (hMGL) catalytic activity, where a critical tryptophan residue acts as a long-range communicator and is essential for maintaining the structure and functional dynamics of hMGL [41]. The HIS208 residue of Ec ProRS was shown to have crucial interactions with the aromatic TYR174 and TYR178 and is critical for maintaining the protein flexibility. Mutation of HIS208 had drastic impact on both flexibility and stability. Similarly, hinge residues as well as the neighboring residues of PBL are crucial to maintain the intrinsic flexibility of Ec ProRS. Taken together, the present work gives additional insights into the role of distal residues in maintaining the flexibility and stability, and therefore, the catalytic activity of ProRSs. As aminoacyl-tRNA synthetases are potential drug targets, the present study may provide alternative drug design possibilities.

Funding This work was supported in part by National Institute of Health [Grant Number: GM117510-01 (S.H.)] and by the Office of Research and Sponsored Programs of the University of Wisconsin-Eau Claire, Eau Claire, WI.

Data Availability The authors confirm that the data supporting the findings of this study within the article [and/or] its supplementary materials will be made available upon request.

Code Availability An online software was used for the present study.

Compliance with Ethical Standards

Conflicts of interest All authors declare that they have no conflict of interest.

References

1. Ibba M, Soll D (2000) Aminoacyl-tRNA synthesis. Annu Rev Biochem 69:617–650
2. Ibba M, Francklyn C, Cusack S (2005) The aminoacyl-tRNA synthetases, Georgetown, TX, USA: Landes Bioscience: Eurekah. com, ©2005
3. Brodkin HR, DeLateur NA, Somarowthu S, Mills CL, Novak WR, Beuning PJ, Ringe D, Ondrechen MJ (2015) Prediction of distal residue participation in enzyme catalysis. Protein Sci 24:762–778
4. Weimer KM, Shane BL, Brunetto M, Bhattacharyya S, Hati S (2009) Evolutionary basis for the coupled-domain motions in *Thermus thermophilus* leucyl-tRNA synthetase. J Biol Chem 284:10088–10099
5. Sanford B, Cao B, Johnson JM, Zimmerman K, Strom AM, Mueller RM, Bhattacharyya S, Musier-Forsyth K, Hati S (2012) Role of coupled dynamics in the catalytic activity of prokaryotic-like prolyl-tRNA Synthetases. Biochemistry 51:2146–2156
6. Johnson JM, Sanford BL, Strom AM, Tadayon SN, Lehman BP, Zirbes AM, Bhattacharyya S, Musier-Forsyth K, Hati S (2013) Multiple pathways promote dynamical coupling between catalytic domains in *Escherichia coli* prolyl-tRNA synthetase. Biochemistry 52:4399–4412
7. Kennedy EJ, Yang J, Pillus L, Taylor SS, Ghosh G (2009) Identifying critical non-catalytic residues that modulate protein kinase A activity. PLoS ONE 4:e4746
8. Ahel I, Stathopoulos C, Ambrogelly A, Sauerwald A, Toogood H, Hartsch T, Soll D (2002) Cysteine activation is an inherent in vitro property of prolyl-tRNA synthetases. J Biol Chem 277:34743–34748
9. Beuning PJ, Musier-Forsyth K (2000) Hydrolytic editing by a class II aminoacyl-tRNA synthetase. Proc Natl Acad Sci USA 97:8916–8920
10. Beuning PJ, Musier-Forsyth K (2001) Species-specific differences in amino acid editing by class II prolyl-tRNA synthetase. J Biol Chem 276:30779–30785

11. Mascarenhas A, Martinis SA, An S, Rosen AE, Musier-Forsyth K (2009) Fidelity mechanisms of the aminoacyl-tRNA synthetases. In: RajBhandary UL, Köhrer C (eds) Protein engineering. Springer Verlag, New York, pp 153–200
12. Cusack S, Yaremchuk A, Krikliviy I, Tukalo M (1998) tRNA(Pro) anticodon recognition by *Thermus thermophilus* prolyl-tRNA synthetase. Structure 6:101–108
13. Stehlin C, Burke B, Yang F, Liu H, Shiba K, Musier-Forsyth K (1998) Species-specific differences in the operational RNA code for aminoacylation of tRNAPro. Biochemistry 37:8605–8613
14. Wong FC, Beuning PJ, Nagan M, Shiba K, Musier-Forsyth K (2002) Functional role of the prokaryotic proline-tRNA synthetase insertion domain in amino acid editing. Biochemistry 41:7108–7115
15. Wong FC, Beuning PJ, Silvers C, Musier-Forsyth K (2003) An isolated class II aminoacyl-tRNA synthetase insertion domain is functional in amino acid editing. J Biol Chem 278:52857–52864
16. An S, Musier-Forsyth K (2004) Trans-editing of Cys-tRNAPro by *Haemophilus influenzae* YbaK protein. J Biol Chem 279:42359–42362
17. An S, Musier-Forsyth K (2005) Cys-tRNA(Pro) editing by *Haemophilus influenzae* YbaK via a novel synthetase.YbaK.tRNA ternary complex. J Biol Chem 280:34465–34472
18. Novoa EM, Vargas-Rodriguez O, Lange S, Goto Y, Suga H, Musier-Forsyth K, Ribas de Pouplana L (2015) Ancestral AlaX editing enzymes for control of genetic code fidelity are not tRNA-specific. J Biol Chem 290:10495–10503
19. Hati S, Ziervogel B, Sternjohn J, Wong FC, Nagan MC, Rosen AE, Siliciano PG, Chihade JW, Musier-Forsyth K (2006) Pretransfer editing by class II prolyl-tRNA synthetase: role of aminoacylation active site in "selective release" of noncognate amino acids. J Biol Chem 281:27862–27872
20. Warren N, Strom A, Nicolet B, Albin K, Albrecht J, Bausch B, Dobbe M, Dudek M, Firgens S, Fritsche C, Gunderson A, Heimann J, Her C, Hurt J, Konorev D, Lively M, Meacham S, Rodriguez V, Tadayon S, Trcka D, Yang Y, Bhattacharyya S, Hati S (2014) Comparison of the intrinsic dynamics of aminoacyl-tRNA synthetases. Protein J 33:184–198
21. Cusack S, Yaremchuk A, Tukalo M (2000) The 2 A crystal structure of leucyl-tRNA synthetase and its complex with a leucyl-adenylate analogue. EMBO J 19:2351–2361
22. Burke B, Lipman RS, Shiba K, Musier-Forsyth K, Hou YM (2001) Divergent adaptation of tRNA recognition by Methanococcus jannaschii prolyl-tRNA synthetase. J Biol Chem 276:20286–20291
23. Stehlin C, Heacock DH 2nd, Liu H, Musier-Forsyth K (1997) Chemical modification and site-directed mutagenesis of the single cysteine in motif 3 of class II *Escherichia coli* prolyl-tRNA synthetase. Biochemistry 36:2932–2938
24. Fersht AR (1975) Demonstration of two active sites on a monomeric aminoacyl-tRNA synthetase. Possible roles of negative cooperativity and half-of-the-sites reactivity in oligomeric enzymes. Biochemistry 14:5–12
25. Liu H, Musier-Forsyth K (1994) *Escherichia coli* proline tRNA synthetase is sensitive to changes in the core region of tRNA(Pro). Biochemistry 33:12708–12714
26. Heacock D, Forsyth CJ, Shiba K, Musier-Forsyth K (1996) Synthesis and aminoacyl-tRNA synthetase inhibitory activity of prolyl adenylate analogs. Bioorg Chem 24:273–289
27. Cestari I, Stuart K (2013) A spectrophotometric assay for quantitative measurement of aminoacyl-tRNA synthetase activity. J Biomol Screen 18:490–497
28. Altschul SF, Madden TL, Schaffer AA, Zhang J, Zhang Z, Miller W, Lipman DJ (1997) Gapped BLAST and PSI-BLAST: a new generation of protein database search programs. Nucleic Acids Res 25:3389–3402
29. Waterhouse A, Bertoni M, Bienert S, Studer G, Tauriello G, Gumienny R, Heer FT, de Beer TAP, Rempfer C, Bordoli L, Lepore R, Schwede T (2018) SWISS-MODEL: homology modelling of protein structures and complexes. Nucleic Acids Res 46:W296–w303
30. Benkert P, Biasini M, Schwede T (2011) Toward the estimation of the absolute quality of individual protein structure models. Bioinformatics 27:343–350
31. Rodrigues CH, Pires DE, Ascher DB (2018) DynaMut: predicting the impact of mutations on protein conformation, flexibility and stability. Nucleic Acids Res 46:W350–w355
32. Humphrey W, Dalke A, Schulten K (1996) VMD: visual molecular dynamics. J Mol Graph 14:33–38
33. Hasegawa H, Holm L (2009) Advances and pitfalls of protein structural alignment. Curr Opin Struct Biol 19:341–348
34. Agarwal PK (2019) A biophysical perspective on enzyme catalysis. Biochemistry 58:438–449
35. Strom AM, Fehling SC, Bhattacharyya S, Hati S (2014) Probing the global and local dynamics of aminoacyl-tRNA synthetases using all-atom and coarse-grained simulations. J Mol Model 20:2245
36. Emekli U, Schneidman-Duhovny D, Wolfson HJ, Nussinov R, Haliloglu T (2008) HingeProt: automated prediction of hinges in protein structures. Proteins 70:1219–1227
37. Walsh JM, Parasuram R, Rajput PR, Rozners E, Ondrechen MJ, Beuning PJ (2012) Effects of non-catalytic, distal amino acid residues on activity of *E. coli* DinB (DNA polymerase IV). Environ Mol Mutagen 53:766–776
38. Richard JP (2019) Protein flexibility and stiffness enable efficient enzymatic catalysis. J Am Chem Soc 141:3320–3331
39. Zhang CM, Hou YM (2005) Domain-domain communication for tRNA aminoacylation: the importance of covalent connectivity. Biochemistry 44:7240–7249
40. Mendonca LM, Marana SR (2011) Single mutations outside the active site affect the substrate specificity in a beta-glycosidase. Biochim Biophys Acta 1814:1616–1623
41. Tyukhtenko S, Rajarshi G, Karageorgos I, Zvonok N, Gallagher ES, Huang H, Vemuri K, Hudgens JW, Ma X, Nasr ML, Pavlopoulos S, Makriyannis A (2018) Effects of distal mutations on the structure, dynamics and catalysis of human monoacylglycerol lipase. Sci Rep 8:1719